Colloid Polym Sci (2006) 285:293–303
DOI 10.1007/s00396-006-1563-y

ORIGINAL CONTRIBUTION

Volume phase transition and structure of poly(*N*-isopropylacrylamide) microgels studied with ^{1}H-NMR spectroscopy in D_2O

Mirja Andersson · Sirkka Liisa Maunu

Received: 10 May 2006 / Accepted: 10 August 2006 / Published online: 5 October 2006

Abstract Thermoresponsive colloidal microgels were prepared by polymerisation of *N*-isopropylacrylamide (NIPAM) with varying concentration of a cross-linking monomer, *N*,*N*-methylenebisacrylamide (MBA), in water with either 0.4 or 6.7 mM concentration of an anionic surfactant, sodium dodecylsulphate (SDS). Volume phase transitions of the prepared microgels were studied in D_2O by ^{1}H-NMR spectroscopy including the measurements of spin–lattice (T1) and spin–spin (T2) relaxation times for the protons of poly(*N*-isopropylacrylamide) (PNIPAM) at temperature range 22–50 °C. In addition, microcalorimetry, turbidometry, dynamic light scattering and electrophoretic mobility measurements were used to characterise the aqueous microgels. The results from the different characterisation methods indicated that PNIPAM microgels prepared in 6.7 mM SDS concentration are structurally different compared to their correspondences prepared in 0.4 mM concentration. Increasing MBA concentration in the microgel synthesis appears to increase the structural heterogeneity in both cases of SDS concentration. PNIPAM structures with significantly higher molecular mobilities at temperatures above 35 °C were observed in the microgels prepared in 0.4 mM SDS concentration, as indicated by the ^{1}H NMR relaxation times of different PNIPAM protons. We conclude that the high mobilities measured with NMR at elevated temperatures and also the clearly negative values of zeta potential are in connection to a fairly mobile surface layer with polyelectrolyte nature and a consequent high local lower critical solution temperature.

M. Andersson (✉) · S. L. Maunu
Laboratory of Polymer Chemistry, Department of Chemistry,
University of Helsinki,
P.O. Box 55, 00014 Helsinki, Finland
e-mail: mirja.andersson@helsinki.fi

Keywords Poly(*N*-isopropylacrylamide) · Microgel · ^{1}H-NMR · Cross-linking density · Structure

Introduction

Poly(*N*-isopropylacrylamide), PNIPAM, phase separates from its dilute aqueous solutions when temperature is raised above its lower critical solution temperature (LCST) at 32 °C [1]. In 1986, the preparation of aqueous, colloidally stable PNIPAM microgel particles showing a rapid volume phase transition upon heating above the LCST was reported for the first time [2], and few years ago, the important developments in the area of thermoresponsive aqueous microgels were reviewed [3]. Still unresolved issues in the preparation and characterisation of PNIPAM microgels are the problems very familiar to all working closely with the aqueous PNIPAM microgel particles such as purification after synthesis, production of very small-sized colloidally stable microgels and the understanding and control of the internal structure of the microgels [4]. The issue of internal structure concerns the microgels prepared by batch copolymerisations of NIPAM and the cross-linking monomer *N*,*N*-methylenebisacrylamide (MBA) in the presence of small amount of surfactant, sodium dodecylsulphate (SDS), or in surfactant-free conditions in water. In aqueous systems, particle production from NIPAM has been shown to proceed via a precipitation polymerisation mechanism as the reaction is conducted above the phase separation temperature and in the presence of MBA. MBA is consumed more rapidly than NIPAM in the polymerisation, indicating the production of particles with heterogeneous internal structure due to nonuniform distribution of cross-links in the radial direction. The role of the surfactant, SDS, in the particle nucleation is to increase

the colloidal stability of precursor particles and thus lower the diameter of primary particles as the number of particles is increased [5]. Many authors have attended to the discussion of the internal structure of PNIPAM microgels during the past few years [6–11], and plenty of evidence have been provided on the heterogeneity of the internal structures. Surprisingly, the preparation of a homogeneous PNIPAM microgel structure (uniform radial cross-linker density) was reported recently. The microgel, synthesised as the heterogeneous ones, but in the presence of high SDS concentration, was studied with small-angle neutron (SANS) and dynamic light (DLS) scattering measurements. The scattering data were consistent with a model of slightly polydisperse spherical particles and homogeneous structure both below and above the phase transition temperature [12].

Structures of corresponding thermoresponsive microgels of another poly(acrylamide)-derivative, poly(*N*-isopropylmethacrylamide), have been studied by liquid-state ^{1}H NMR with relaxation measurements [13], but there are only few reports of applying the liquid-state NMR, as more than a method of chemical analysis, in the studies of PNIPAM microgels. Solvent diffusion measurements at various temperatures by the pulsed-gradient spin-echo (PGSE)-NMR have been reported, and more recently, the same approach was used to study the effect of the cross-linker (MBA) concentration on the volume phase transition of PNIPAM microgels [14, 15]. The influence of the MBA concentration in the microgels prepared in zero/low SDS concentrations has been studied mainly by other methods [6, 7, 16–21]. The application of ^{1}H NMR spectroscopy to investigate the phase transition [22–26] is rather seldom. Spevacek and coworkers have done systematic work to study the phase separation of other thermoresponsive polymers [27–31] and also linear PNIPAM [32] in D_2O by measuring temperature dependences of the ^{1}H NMR spectra and the ^{1}H NMR relaxations. We have applied similar methodical approach in a recent study of cross-linked PNIPAM on 50-nm-sized polystyrene latex particles. The volume phase transitions of nano-sized PNIPAM gel layers on solid core particles were analysed with NMR in D_2O in comparison to microgel samples, and complementing information of the phase transitions on molecular level was obtained by microcalorimetry [33]. The lack of better knowledge on PNIPAM microgels was noticed as a problem, and more information on the temperature dependence of the ^{1}H NMR spectra and the ^{1}H NMR relaxations of PNIPAM microgels was needed.

The study reported here was motivated by the ongoing discussion on the structural features of the PNIPAM microgels. The aim of the present work was to study the PNIPAM microgel structures synthesised with different concentrations of the cross-linking monomer, MBA, in the presence of both small and large amount of surfactant, SDS, by measuring the temperature dependences of both the ^{1}H NMR spectra and the ^{1}H NMR relaxations of PNIPAM microgels. In addition, microcalorimetry, turbidometry, DLS and electrophoretic mobility measurements were used to get information on the aqueous microgels at different temperatures. More detailed investigation on the influence of the SDS concentration in the microgel synthesis will be reported later.

Experimental

Materials and syntheses

N-isopropylacrylamide (NIPAM; Acros) was recrystallised from *n*-hexane and dried in vacuum. Sodium dodecylsulphate (SDS; Merck), potassium peroxydisulphate (KPS; Merck) and *N*,*N*-methylenebisacrylamide (MBA; Aldrich) were used as received. Water used in syntheses and characterisations was deionised by using Elga PurelabUltra-equipment. Filter papers (Whatman, 2V) used were of pore size 8 μm. Cellulose membrane tubings (CelluSep T4) with nominal molecular weight cut-off 12,000–14,000 g/mol were used as membranes in microgel purification by dialysis. A summary of the syntheses and the abbreviations for the microgels are shown in Table 1. Polymerisations were carried out in a sealed round-bottom flask equipped with a magnetic stirrer and an oil bath to control the reaction temperature. In a typical synthesis, NIPAM and MBA were separately dissolved in premade aqueous solution of SDS, and both solutions were transferred into the reaction flask. The flask was sealed with a septum, and the solution was purged with nitrogen and stirred at room temperature for 20 min. The nitrogen inlet and outlet were removed and the flask was placed into a preheated oil bath at 70 °C. Polymerisation was initiated after stirring (650 rpm) for 20 min by injecting KPS, dissolved in 2 ml of water, to the reaction mixture. Total amount of water used in a polymerisation batch was typically 20–26 ml. The reaction was allowed to proceed in stirring for 4 h. The reaction was stopped by unsealing the flask and cooling the product to room temperature. The product was filtered through a filter paper. The aqueous microgel dispersions were purified by dialysis for 7 days against distilled water that was refreshed daily (twice during the first 3 days). The purified dispersions were stored as such in the refrigerator. Polymer contents of aqueous microgel dispersions were obtained by drying weighed samples of aqueous dispersions to equilibrium weight in vacuum.

Table 1 Preparation of the microgel samples and the measured values of hydrodynamic radius and zeta potential above and below the cloud point of PNIPAM

Sample	MBA (mM)	SDS (mM)	R_h[a], 20 °C (nm)	R_h[a], 50 °C (nm)	ζ[b], 20 °C (mV)	ζ[b], 40 °C (mV)
M1.6	1.6	0.4	200	92	−2.4 (±6%)	−40.7 (±4%)
M3.2	3.2	0.4	196	101	−4.1 (±5%)	−41.2 (±3%)
M6.5	6.5	0.4	190	100	−15.0 (±5%)	−37.6 (±4%)
M13	13	0.4	202	126	−15.5 (±4%)	−40.2 (±4%)
M4.2S	4.2	6.7	35	19	+2.1 (±7%)	−0.8 (±7%)
M6.5S	6.5	6.7	47	21	+1.8 (±7%)	−1.2 (±7%)
M8.4S	8.4	6.7	54	22	+1.4 (±8%)	−0.7 (±8%)
M13S	13	6.7	44	29	+1.1 (±8%)	−1.9 (±7%)

In the synthesis batches: NIPAM, 130 mM; KPS, 2 mM; and water, 20–26 ml (total amount).
[a] Hydrodynamic radii (mean, deviation <±8%) from size distributions (DLS, intensity-weighed) in H_2O.
[b] Zeta potentials (mean from six measurements) by Zetaziser in H_2O.

Characterisation methods

The size distributions of particles at various temperatures (20–50 °C) were measured with DLS by using the instrument of Bookhaven Instruments (BI-200SM goniometer, BI-9000AT digital correlator) equipped with an argon laser at wavelength 488 nm. Scattering was measured at 90° angle and the obtained time correlation functions were analysed by CONTIN Laplace-inversion program. The polymer concentrations in the samples were 0.01–0.1 g/l obtained by diluting the dialysed particle dispersions with deionised water. Temperature of the sample unit was controlled with Lauda RC6 CP-thermostate.

The zeta potentials of the aqueous microgel samples were measured using a zeta potential analyser (Malvern Zetasizer 3000HSA, Malvern Instruments) at temperatures 20 and 40 °C. Samples were prepared by redispersing freeze-dried microgels in deionised water. Polymer concentrations in aqueous dispersions used in the measurements were 0.1–1 g/l. Electrophoretic mobilities (depending on the sizes and charges of the analytes and on the type of the solvent) of the microgels in aqueous dispersion were first measured and the zeta potentials (ζ) were calculated from the mobilities with the software supplied by the Zetasizer manufacturer using the Smoluchovski approximation of the Henry function. The Smoluchovski approximation gives the most accurate approximations of the zeta potentials in the cases where the particle sizes are >100 nm in aqueous solutions with ionic strengths $>10^{-3}$ M.

The change of optical density (absorbance) of the aqueous dispersions of the microgels was monitored at a wavelength of 500 nm with a UV–Vis spectrophotometer (Shimadzu 1601PC) as a function of temperature. The temperature of the sample unit was controlled with Huber Ministat-thermostate programmed to heat at a rate of 12 °C/h from 20 to 50 °C. The polymer concentrations in the samples were 1 g/l and the samples were prepared from freeze-dried polymers.

High-sensitivity differential scanning calorimetry (HS DSC) measurements were performed with a VP-DSC microcalorimeter (Microcal Inc.) at an external pressure of approx 180 kPA. The cell volume was 0.507 ml. Scans were recorded from 10 to 80 °C at heating rates 30 and 60 °C/h. Prior to each scan, the sample was kept at 10 °C for 15 min and each scan was repeated three times. Data were analysed by using the software supplied by the manufacturer. The raw data from HS DSC were corrected by subtracting the baseline and the sample concentration was given as molar concentration of NIPAM units in the particle sample. The samples were prepared from freeze-dried microgels by redispersing in H_2O. The polymer concentration was 1 g/l.

^{1}H NMR spectra and relaxation measurements of the particles in D_2O were measured using a Varian UNITYI-NOVA spectrometer operating at 300 MHz for protons equipped with a temperature control unit. The NMR samples were prepared by redispersing 20 mg of freeze-dried particles in 1 ml of D_2O and were filtered through a filter paper. Measurements were carried out with controlled heating and cooling steps, allowing the samples to equilibrate for 30 min at each incremented temperature. For the ^{1}H T1 relaxation measurements of the polymer protons, a series of ~30 spectra were collected using the standard inversion recovery sequence varying the delay time from 0.001 to 10 s. The ^{1}H T2 relaxation measurements of the polymer protons were made using the Carr-Purcell-Meiboom-Gill spin-echo sequence using an array of ~20 values ranging from 0.002 to 1 s. The T1 and T2 relaxation times were obtained by fitting a monoexponential decay to the relaxation data. The errors of the monoexponential fits in the exponential data analysis were typically <1% for T1s at temperature ≤35 °C and <3% at the higher temperatures. The corresponding errors of the

exponential data analysis for T2s were at maximum 6% at temperature ≤35 °C and <10% at the higher temperatures.

Results and discussion

The recipes reported by Wu et al. [5] were applied in the preparation of the microgel samples for this study (see Table 1). The highest SDS concentration reported in the case of Wu et al. was 4 mM, but usually, the surfactant concentration in their study was 10 times lower. At SDS concentration range 0.2–4 mM, a dependence of the hydrodynamic diameter of microgel (volume averaged by DLS at 50 °C) from the SDS molarity has been found to follow the equation:$\log(\text{diameter, nm}) = -0.71 * \log(\text{SDSmolarity})$[5]. Recently, Arleth et al. [12] reported the use of 5.3 mM SDS concentration in microgel preparation and a resulting small-sized (R_h approx 50 nm at room temperature), structurally homogeneous (uniform radial cross-linker density) aqueous microgel structure, as indicated by the data from their SANS measurements below and above the phase transition temperature. In our study, a group of microgels was prepared in an even higher SDS concentration compared to that in Ref. [12], in 6.7 mM concentration (see Table 1), but still in the condition below the critical micelle concentration of SDS (CMC in water approx 8 mM at room temperature).

It is known that the cloud point of linear PNIPAM in water increases significantly in the presence of SDS. The ionic surfactant binds to the polymer resulting in the formation of a charged polymer–surfactant complex. The electrostatic repulsion between the charged complexes prevents the aggregation of polymer chains effectively above the LCST, especially when the polymer concentration is low. Consequently, polymer precipitation is affected by SDS [34].

The mean hydrodynamic radii and the size distributions in dilute aqueous dispersions of the microgels were obtained from the DLS data at various temperatures (20–50 °C). The mean hydrodynamic radii, R_h, from the intensity-weighed size distributions of the microgel samples at 20 and 50 °C are shown in Table 1. As expected, the increase in the SDS concentration in the polymerisation batch decreases the hydrodynamic size of the microgel, but also the polydispersity of the product microgel appears to be increasing as could be concluded from the size distributions measured with DLS (size distributions are not shown here). All the microgel samples decrease in hydrodynamic size (Table 1) upon heating from 20 to 50 °C due to the volume phase transition occurring at temperatures close to the LCST of PNIPAM. The size distributions in all cases remained monomodal and coagulation was not observed during the measurements above the phase transition temperature. DLS data upon cooling were also measured (not shown), and for all the samples, the deswelling was observed to be reversible. The microgels are most likely stabilised against coagulation at elevated temperatures by electrostatic repulsion between the anionic surface groups originating from the polymerisation initiator fragments and the residual surfactant. This assumption is supported by the measured negative values of zeta potential (ζ) at 40 °C for the aqueous microgels also listed in Table 1. In all cases, the value of zeta potential becomes more negative as the temperature is increased above the LCST of PNIPAM. Our results are consistent with the reports that the electrophoretic mobility of PNIPAM microgel particles in water (colloidally stabilised by charges) increases as temperature is raised from 20 to 40 °C [8, 16, 35]. The lowest values of zeta potential at 40 °C (approx −40 mV as shown in Table 1) were observed for the samples prepared with the low concentration of SDS, whereas the microgels prepared in 6.7 mM SDS concentration show only slightly negative values. Daly and Saunders have reported a zeta potential of approx −38 mV measured with a corresponding method (calculated from the electrophoretic mobilities using the Smoluchovski approximation) at 46 °C for an aqueous PNIPAM microgel particle (R_h approx 500 nm at 25 °C). The particles were electrostatically stabilised by the negative charges from the polymerisation initiator fragments. In particle preparation, they used the surfactant-free method [36]. In our case, the values of the zeta potentials show a clear difference between the microgels prepared with the low and the high surfactant concentration.

Figure 1a presents the changes of optical densities (measured absorbance) versus temperature in the aqueous microgel samples with equivalent polymer concentrations (1 g/l). Only the data for the microgels prepared in 6.7 mM SDS concentration are shown. In all cases, an increase in the absorbance is observed upon heating. However, very low turbidities (absorbances <0.05 in Fig. 1a) were observed for these microgels compared to the microgels prepared in 0.4 mM SDS concentration. In an corresponding experiment, for loosely cross-linked sample prepared in 0.4 mM SDS concentration (sample M1.6), much higher absorbances of 0.2 and 1.2 were measured at temperatures 20 and 50 °C, respectively. The turbidity curve of M1.6 (1 g/l) is not included in Fig. 1a due to the completely different level of absorbance compared to the other samples presented. The other microgels prepared in 0.4 mM were not studied with turbidometry since there are more sensitive methods available to study the phase transitions of high turbidity samples. In this study, the high turbidity indicates the presence of significant fraction of permanent, solid particle structures evolved during the precipitation cross-linking polymerisation. High SDS concentration in the synthesis batch is concluded to prevent the formation of permanent, solid

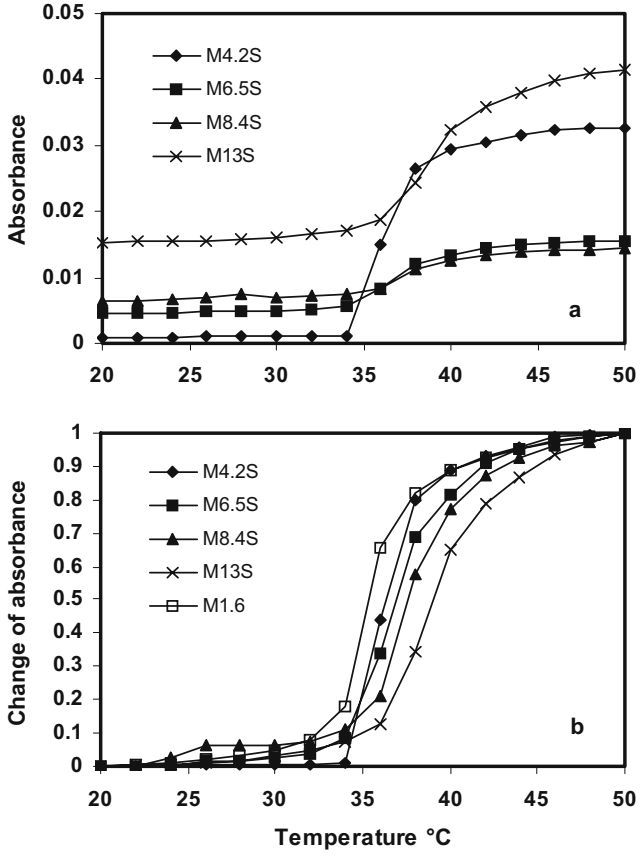

Fig. 1 **a** The change of optical density (measured absorbance at λ= 500 nm, experimental errors <0.005) with temperature for different microgels (1 g/l in H_2O, heating rate 12 °C/h). **b** The normalised change of optical density (from absorbance at λ=500 nm) with temperature for different microgels (1 g/l in H_2O, heating rate 12 °C/h)

PNIPAM particles that would cause permanent turbidity of the aqueous dispersions. Turbidity observed at temperatures below the cloud point of PNIPAM increases with increasing cross-linker concentration in Fig. 1a. Evidently, more solid particle structures are formed with large amounts of MBA. To compare the changes of turbidity with temperature for different microgels, the normalised changes of optical densities with temperature are shown in Fig. 1b. In this case, the measured absorbance values at 20 °C were taken as points of zero and the absorbance values were divided with the highest absorbance to normalise the data. According to the turbidity from the microgels prepared in 6.7 mM SDS solution, the phase transition shifts towards higher temperatures and broadens with increasing cross-linker concentration. The normalised turbidity data from the microgel M1.6, prepared with the lower SDS concentration, are plotted in Fig. 1b for comparison. M1.6 shows fairly broad phase transition, although the MBA concentration used in its synthesis was low.

The calorimetrically obtained transition temperature of PNIPAM-based polymers is often defined as the onset of the DSC transition endotherm, T_{onset} (the intersection of the baseline and the leading edge of the endotherm). The temperature of the maximum heat capacity (T_{max}) is also used to describe the transition temperature. For a sharp peak in a DSC thermogram, it is possible to determine T_{onset} very precisely. However, for broad peaks, the determination of T_{onset} is more difficult due to inaccuracy in setting the baseline, and in such cases, it appears to be more reliable to determine the T_{max} in comparative studies. The thermodynamic parameters of the volume phase transitions (dehydration of PNIPAM) at heating rate 30 °C/h for the prepared microgels are reported here. The transition temperatures (T_{max}) versus MBA concentration in the synthesis are presented in Fig. 2a. The T_{max} increases with increasing cross-linker concentration, and the effect appears to be more pronounced in the case of the microgels prepared with the high SDS concentration. Higher transition temperatures are observed for the microgels prepared in 6.7 mM surfactant solution. However, it seems that the purified microgels do not contain very large amounts of residual SDS, although the purification was conducted only by dialysis since the transition temperatures are not more increased by the high SDS concentration in the polymerisation batch. The effect of added SDS to the dehydration of aqueous PNIPAM microgels has been studied microcalorimetrically by others. At heating rate 60 °C/h and with polymer concentration 0.48% in water, the measured values of T_{max} were 35.0, 35.8 and 45.6 °C in SDS concentrations 0, 2 and 6 mM, respectively [37].

The microcalorimetric thermograms were recorded also by using a higher heating rate, 60 °C/h. Higher values of T_{max} (0.1–0.5 °C) and slightly broader endotherms of dehydration were obtained with the higher heating rate (data not shown). Recently, Ding and coworkers [38] reported similar effects of heating rate to the microcalorimetric data of linear PNIPAM (M_w=1.6*10^6 g/mol) in water. Similar HS DSC results as function of heating rate have been obtained also for 10-μm-sized PNIPAM gel (MBA as cross-linker) particles suspended in water [39]. The gels were prepared in the good-solvent conditions and their structure can be assumed to be more homogeneous compared to microgels prepared in the poor-solvent conditions. Both samples, the linear PNIPAM [38] and the PNIPAM hydrogel [39], gave considerably more narrow endotherms of dehydration than were measured for PNIPAM microgels with various cross-linker (MBA) densities by Woodward and coworkers [15]. Also, in our case, the measured endotherms of dehydration were fairly broad in all cases, indicating certain level of heterogeneity in all the microgels, but smaller values for the width of the transition at half-height ($\Delta T_{1/2}$) are observed for the microgels prepared at the high SDS concentration compared to the low SDS concentration as shown in Fig. 2b. Clearly, the

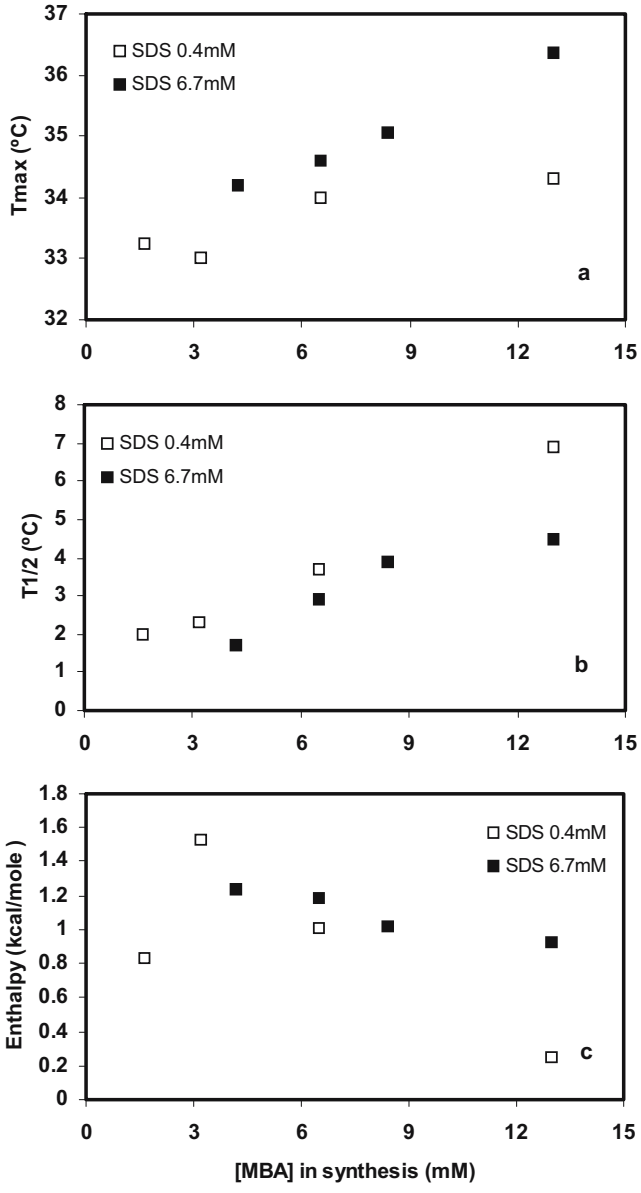

Fig. 2 Thermodynamic parameters of volume phase transition measured with microcalorimetry from the aqueous microgels (1 g/l, heating rate 30 °C/h). The temperature of the maximum heat capacity (**a**; T_{max}, maximum errors ±0.3%), the width of the transition at half-height (**b**; $\Delta T_{1/2}$, maximum errors ±0.3%) and the calorimetric enthalpy of transition, ΔH_{cal} (**c**; per moles of NIPAM units, maximum errors ±4%) versus MBA concentration in the synthesis batch

width of the transition increases with the increasing cross-linker concentration in both cases of SDS concentration. The values of calorimetric enthalpy of transition, ΔH_{cal} (per moles of NIPAM units), are correspondingly plotted against MBA concentration in the synthesis in Fig. 2c. ΔH_{cal} decreases significantly with MBA concentration with the microgels prepared in 0.4 mM SDS solution. With the higher SDS concentration, the corresponding effect of cross-linker concentration is not so significant but, in any case, clearly observable. Very low enthalpy of dehydration per NIPAM units, observed for the sample prepared in 0.4 mM SDS concentration with the highest amount of MBA, indicates the presence of significant fraction of insoluble/non-hydrated PNIPAM in the microgel structure.

PNIPAM microgels with various cross-linking densities (0.7–11 mol% of the monomers in synthesis) have been studied by Kratz and coworkers. They used several characterisation methods such as DLS, SANS, electron and atomic force microscopy [7]. The swelling ratio was observed to decrease with increasing MBA concentration, which was attributed to the topological constraints introduced through an increasing number of cross-linking points. It was concluded from their SANS data that the polymer network in the swollen state becomes more heterogeneous with increasing cross-linker concentration. Interestingly, based on the deswelling behaviour (DLS) as a function of temperature, it was concluded that the transition temperature does not change significantly with cross-linker concentration, and it was claimed that the thermodynamics of the process is not affected by the cross-linker density. The transition temperatures in their case were given by the inflection points of the derivatives of the deswelling curves: R_h (at temperature x)/R_h (in the swollen state at 15 °C) versus temperature. However, broadening of the transition with increasing cross-linker concentration was observed [7]. The transition broadening and the decrease in swelling ratio with increasing cross-linking density were also observed in a light scattering study by Varga and coworkers [6]. They prepared the microgels based on the recipes of Wu et al. [5] in low SDS concentration (<1 mM) with varying MBA concentrations (<10 mol% of the monomers in synthesis). The structure of the microgel particles was found to strongly depend on the degree of cross-linking. In the swollen state, the mean polymer density inside the microgel increased significantly with the cross-linker concentration, whereas in the collapsed state, only a slight increase could be observed. They suggested that with increasing amount of the cross-linker, the size of a strongly cross-linked core increases and the structure of the microgel particles gradually shifts from a loose network/highly branched polymer with the coil-like nature observed with DLS to a compact gel particle possessing a nonuniform segment density distribution inside and possessing a surface layer with very low cross-link density [6]. Woodward and coworkers have used methodical combination similar to our study to characterise PNIPAM microgels with various cross-linking densities. In their case, microgels were prepared in the surfactant-free conditions and by using MBA 0.25–30% of monomers in the polymerisations. Turbidometric, light scattering and high-sensitivity DSC analyses showed that the temperature and the width of volume phase transition increase with the increasing

cross-linker concentration. Our results of microgels prepared in SDS solutions appear to be in good accordance with their results. They reported also the results of the PGSE-NMR diffusion measurements in D_2O, where the diffusion of the solvent molecules within the microgels was studied. The rate of solvent diffusion within the microgels decreased with the increasing cross-linking density [15].

The ^{1}H NMR investigations

We studied the volume phase transition of PNIPAM microgels on molecular level with quantitative ^{1}H NMR spectroscopy in D_2O by monitoring the polymeric protons. By NMR in liquid state, we can study the mobile/soluble structures, and possible solid structures in samples cannot be analysed. Typical ^{1}H NMR spectra of a PNIPAM microgel in D_2O below and above the LCST are presented in Fig. 3. The chemical structure of a NIPAM unit is included in the figure. Figure 4a shows the curves of the normalised PNIPAM proton (methyl proton from the side chain at approx 1 ppm) to solvent proton (4.8 ppm) spectral intensity ratios versus temperature (22–50 °C) for the microgels synthesised in 0.4 mM SDS concentration. As expected, dramatic decrease in the PNIPAM proton signal intensities occurs during the phase transition. The signals become hardly detectable by liquid-state NMR as the transition has taken place, and at temperatures above 35 °C, we are most likely observing proton signals only from the surface (still soluble/mobile structures) of the collapsed particle. The intensity data from the side chain protons in Fig. 4a suggest that the phase transition is not significantly affected by the MBA concentration. However, the corresponding data obtained by monitoring the methyne protons in the main chain (2 ppm) in Fig. 4b suggest otherwise. The increasing MBA concentration decreases significantly the response temperature of the main chain

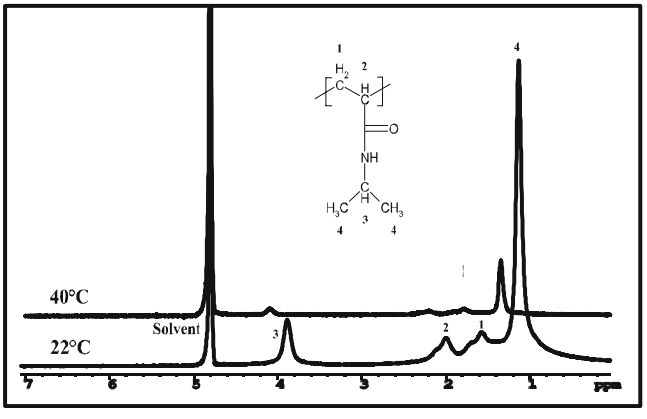

Fig. 3 Typical ^{1}H NMR spectra of PNIPAM microgel at 22 and at 40 °C in D_2O (recorded with the microgel sample M1.6)

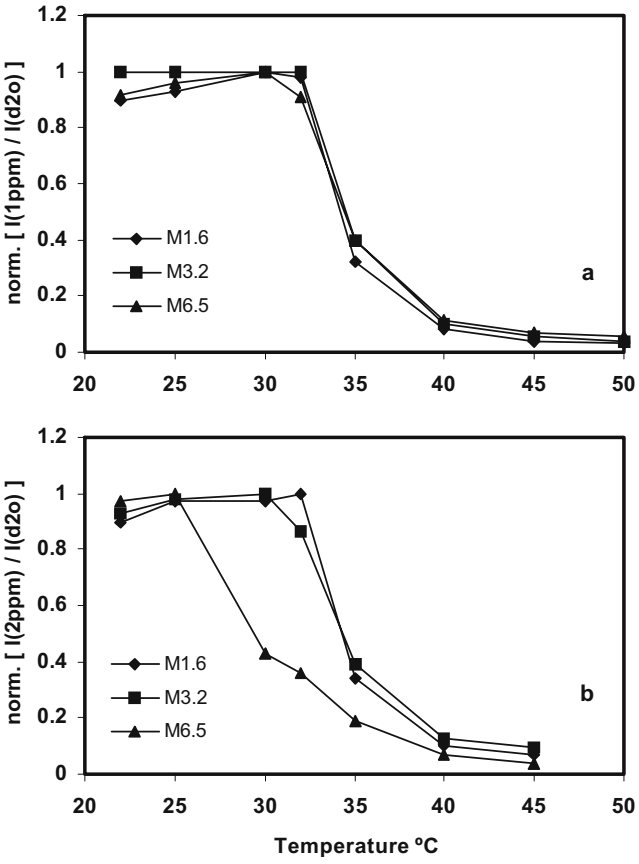

Fig. 4 Normalised ratios of the ^{1}H NMR signal intensity (*I*) of the methyl protons (**a**; side chain, approx 1 ppm) and methyne protons (**b**; main chain, approx 2 ppm) to the solvent (D_2O, approx 4.8 ppm) protons versus temperature in different samples

protons of sample M6.5, and the decrease in intensity of the proton signals occurs at broader temperature range. Peculiarly, corresponding different response of the main chain and the side chain signals connected to the cross-linker concentration was not observed in the sample set prepared in 6.7 mM SDS concentration, but the temperature response curves of the main and side chain protons were found nearly identical (data not shown). Correspondingly to our earlier results [33], a slight increase in the signal intensities in Fig. 4(a,b) is observed for some samples as heated below the transition temperature. This increase in intensities could be interpreted as being due to increasing mobility with increasing temperature below the phase transition temperature. Corresponding observations have also been reported by Zhu and Napper for ^{13}C NMR signals from linear PNIPAM chains both in solution and attached to polystyrene latex particles [40].

Dynamic behaviour of PNIPAM chains in the microgels was studied by measuring spin–lattice (T1) and spin–spin (T2) relaxation times of the side chain and the main chain protons at temperatures 22–50 °C in D_2O.

The relaxation decays were monoexponential in all cases indicating that we were monitoring only the most mobile segments in all the samples. This means that signal from the significantly less mobile parts of the polymers is not reflected in the relaxation data. When analysing the structural connections of the relaxation times, the broad temperature range of study can be divided in two parts. We assume that at temperatures above 32–35 °C, we are monitoring only the surface (with high molecular mobility) of the collapsed microgels. The values of T1 of the side chain methyl protons versus temperature are shown in Fig. 5a. It appears that T1 of the methyl protons is not highly sensitive to structure of a microgel since close values of T1 were obtained for all samples at the same temperature at range 22–35 °C. The accuracy of the relaxation times is fairly low at temperatures above 35 °C due to the decreasing intensity of the proton signals; however, increasing trend of T1 for the side chain methyl protons with temperature is observed for all the studied samples at the studied temperature range, 22–50 °C. The increase in T1 with temperature, as the spin–lattice relaxation slows down, is concluded to be due to decreasing mobility during the phase transition. The T1 relaxation times versus temperature for the main chain methyne protons in the microgels prepared in 0.4 mM SDS concentration are shown in Fig. 5b. At temperatures 22–35 °C, T1 decreases with decreasing cross-linker concentration indicating higher mobility in the loosely cross-linked microgels. For all samples, T1 clearly starts to increase when the phase transition temperature is reached. According to these data, in the case of M1.6, the increase in T1 is observed at quite high temperatures, above 40 °C. The high response temperature observed for M1.6 may reflect a higher local phase transition temperature of charged PNIPAM chains on the surface of microgel particle. Evidences of the coronal polyelectrolyte layers with high local LCSTs in PNIPAM microgels have been reported [8]. Furthermore, in the case of M3.2, T1 values can be analysed at high temperatures since the proton signals from the main chain are still observable as small ones. For the microgels in H_2O, the strongly negative values of zeta potential were obtained at 40 °C (see Table 1), which supports the assumption of surface with polyelectrolyte nature in these cases. Whereas for the microgels synthesised in 6.7 mM SDS concentration and showing zeta potentials closer to zero at 40 °C, the T1 values of the corresponding main chain signal cannot be properly analysed at temperatures above 40 °C since the proton signals disappear completely upon heating as shown in Fig. 5c. Also, in this sample set, the highest value of T1 (the lowest mobility) is observed for the tightly cross-linked microgel (M13S) at temperatures below 35 °C.

The spin–spin relaxation times (T2) of the side chain methyl protons in the microgels prepared in 0.4 mM SDS

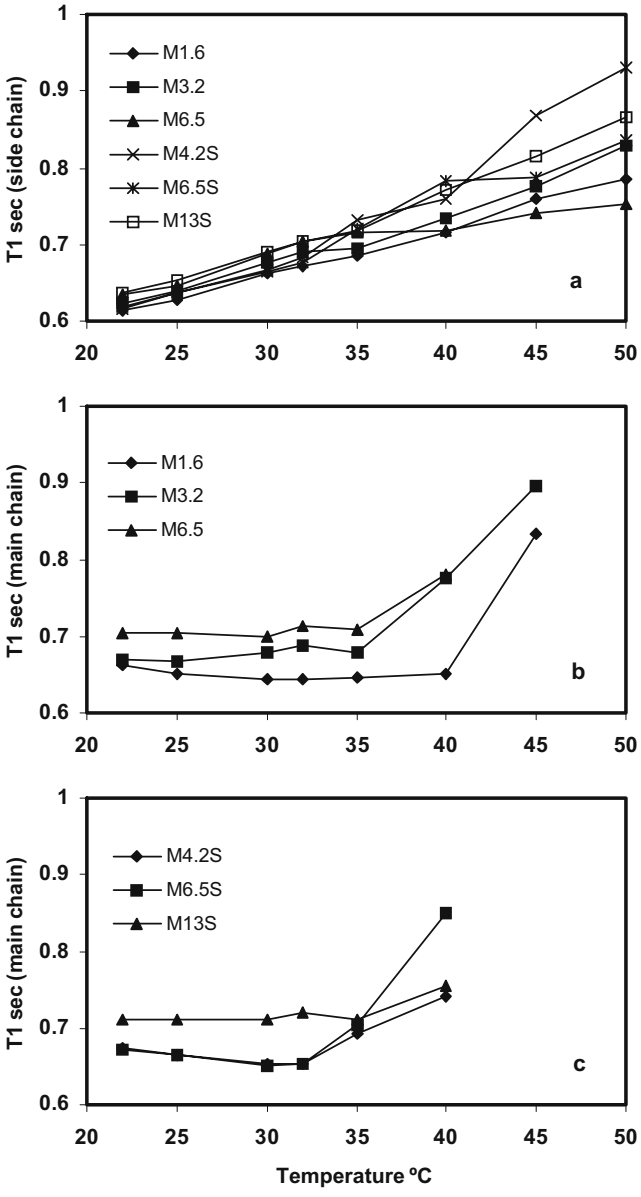

Fig. 5 ^{1}H NMR relaxation times measured from the microgels in D_2O. Spin–lattice relaxation times (T1) of the methyl protons (**a**; side chain, approx 1 ppm). Spin–lattice relaxation times (T1) of the methyne protons (main chain, approx 2 ppm) for the microgels prepared in 0.4 mM (**b**) and in 6.7 mM (**c**) SDS solution

concentration are shown in Fig. 6a. Higher values of T2 (higher mobilities) are observed for the samples with low cross-linking density. The values of T2 show shifts upwards at 35 °C. In Fig. 6b, the corresponding data for the sample set prepared in 6.7 mM SDS concentration are shown and decreasing T2s upon heating are observed. The decreasing T2 with increasing temperature is concluded to reflect the decreasing mobility of the side chain groups on the phase transition. At temperatures 22–32 °C, the T2 decreases (mobility decreases) with the increasing cross-linker concentration. The microgel M13S, the tightly cross-linked sample,

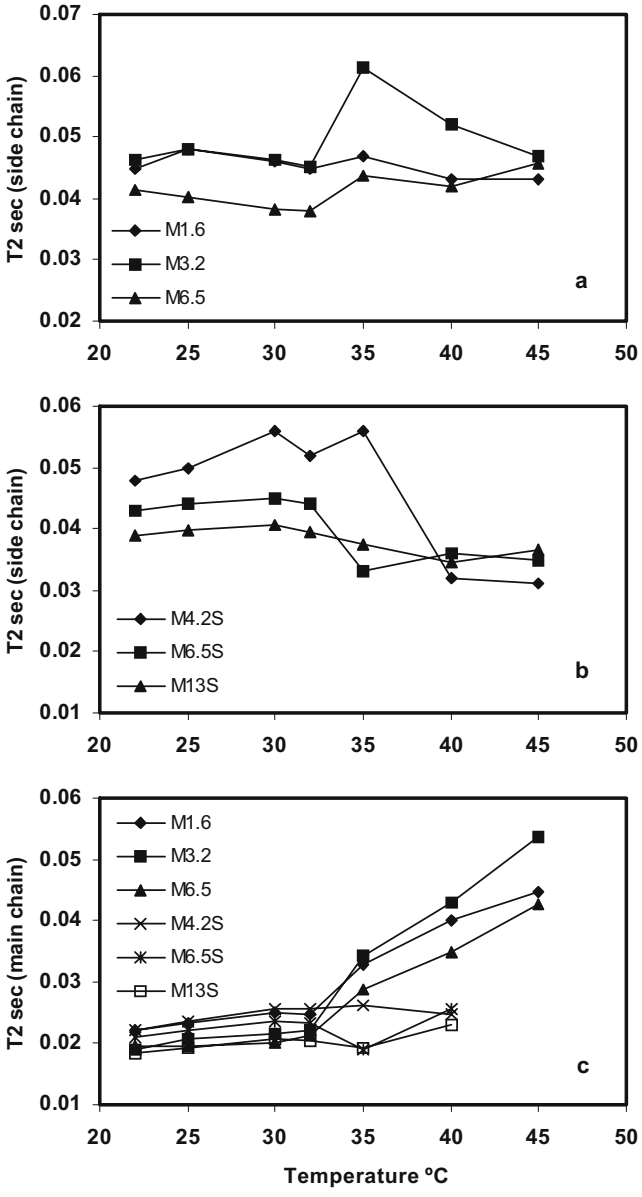

Fig. 6 ^{1}H NMR relaxation times measured from the microgels in D_2O. Spin–spin relaxation times (T2) of the methyl protons (side chain, approx 1 ppm) for the microgels prepared in 0.4 mM (**a**) and in 6.7 mM (**b**) SDS solution. Spin–spin relaxation times (T2) of the methyne protons (**c**; main chain, approx 2 ppm)

shows quite a small change of mobility with temperature compared to the other two microgels. At high temperatures (40–45 °C), the mobilities are significantly higher for the samples prepared in the low SDS concentration as shown in Fig. 6a. The T2 values versus temperature for the methyne protons in the main chain for the microgels are presented in Fig. 6c. The microgels prepared in 0.4 mM concentration of SDS show clearly a step of T2 towards higher values as temperature exceeds 32 °C, whereas the samples prepared in 6.7 mM SDS concentration do not show such response. As in the case of T1 for the corresponding proton signals in Fig. 5c, the T2 values of the microgels prepared in 6.7 mM SDS concentration cannot be analysed above 40 °C due to the disappearance of the proton signals. The higher mobilities observed in the samples prepared in the low SDS concentration at temperatures above 32 °C in Fig. 6c are again interpreted to be in connection to a mobile surface layer with polyelectrolyte nature.

The results from the different characterisation methods in this study indicate that the PNIPAM microgel structures prepared in 6.7 mM SDS concentration are different from their correspondences prepared in 0.4 mM surfactant concentration. Recently, Arleth et al. [12] reported the structurally homogeneous (uniform radial cross-linker density) aqueous microgel prepared in 5.3 mM SDS solution, as indicated by the data from their SANS measurements below and above the phase transition temperature. Our results show that increasing MBA concentration in the microgel synthesis increases the structural heterogeneity in both SDS concentrations. The increase in structural heterogeneity with increasing MBA density has already been reported by several authors in the cases of PNIPAM microgels prepared in zero/low SDS concentrations. The high turbidities typically observed in aqueous dispersions of PNIPAM microgels, prepared in zero/low SDS concentrations, lead to think that there are solid structures (unhydrated PNIPAM) present also in the good-solvent conditions. It is logical that large amounts of SDS in the precipitation polymerisation batch may prevent he formation of tightly packed PNIPAM aggregates that would eventually form the permanent, solid PNIPAM particles due to cross-linking. We believe that PNIPAM microgels prepared in zero/low SDS concentrations in the swollen state possess a nearly unhydrated, solid core, and the size and the solid nature of the core increase with increasing cross-linking concentration in the polymerisation batch. The observed decreasing phase transition enthalpies with increased cross-linking also point out to the increasing fraction of unhydrated structures. Furthermore, on the nearly unswellable core, there is the highly swellable shell, where the cross-linking density possibly decreases towards the particle surface and some dangling PNIPAM chains on the particle surface form a coronal layer. The colloidally stabilising charges enrich to the outermost part of PNIPAM microgel particle on the synthesis conditions giving a polyelectrolyte nature to the surface layer as already suggested by others [8].

Conclusions

In this study, we investigated aqueous PNIPAM microgels prepared by precipitation polymerisation method in two SDS concentrations (0.4 and 6.7 mM) and varying

the amount of *N*,*N*-methylenebisacrylamide (MBA) as the cross-linking monomer. The microgels were characterised on particle level with turbidometry, DLS and zeta potential measurements. Turbidity of the aqueous microgel dispersions in the good-solvent conditions was found to be significantly higher when the low SDS concentration was used in the microgel synthesis. High SDS concentration in the polymerisation batch is concluded to prevent the formation of permanent, solid PNIPAM particle structures that would cause permanent turbidity of aqueous microgel dispersion. Turbidity observed at temperatures below the cloud point of PNIPAM increases with increasing cross-linker concentration. Evidently, more solid particle structures are formed with large amounts of MBA.

On molecular level, the microgels were studied with microcalorimetry in H_2O and with high-resolution ^1H NMR in D_2O. The phase transition temperature increases with increasing cross-linker concentration, and the effect appears to be more pronounced in the case of the microgels prepared with the high SDS concentration, as indicated by the results from microcalorimetry. The width of the transition increases with the increasing cross-linker concentration in both cases of SDS concentration. The value of calorimetric enthalpy of the phase transition decreases significantly with MBA concentration with the microgels prepared in the low SDS solution. Corresponding effect of cross-linker concentration was not so significant with microgels prepared in the high SDS concentration but, in any case, clearly observable. Low enthalpy of dehydration per NIPAM units indicates the presence of significant fraction of insoluble/non-hydrated PNIPAM in the microgel structure. PNIPAM structures with significantly higher mobilities at temperatures above 35 °C were observed in the microgels prepared in low concentration of SDS, as indicated by the ^1H NMR relaxation times of different PNIPAM protons. We conclude that the high mobilities measured with NMR at elevated temperatures, and also the clearly negative values of zeta potential in H_2O, are in connection to a fairly mobile surface layer with polyelectrolyte nature and a consequent high local LCST. At temperatures 22–35 °C, the spin–lattice relaxation times (T1s) of PNIPAM protons indicated increasing mobility of PNIPAM chains with decreasing cross-linker concentration. Corresponding observation was also made by analysing the spin–spin relaxation times (T2s) at temperatures 22–32 °C.

References

1. Heskins M, Guillet JE (1968) J Macromol Sci Chem A2:1441
2. Pelton RH, Chibante P (1986) Colloids Surf 1986 20:247
3. Pelton R (2000) Adv Colloid Polym Interface Sci 85:1. DOI 10.1016/S0001-8686(99)00023-8
4. Pelton R (2004) Macromol Symp 207:57. DOI 10.1002/masy.200450306
5. Wu X, Pelton RH, Hamielec AE, Woods DR, McPhee W (1994) Colloid Polym Sci 272:467
6. Varga I, Gilanyi T, Meszaros R, Filipsei G, Zrinyi M (2001) J Phys Chem B 105:9071. DOI 10.1021/jp004600w S1089-5647(00)04600-9
7. Kratz K, Hellweg T, Eimer W (2001) Polymer 42:6631. DOI 10.1016/S0032-3861(01)00099-4
8. Daly E, Saunders BR (2000) Phys Chem Chem Phys 2:3187. DOI 10.1039/b002678f
9. Saunders BR (2004) Langmuir 20:3925. DOI 10.1021/la036390v S0743-7463(03)06390-X
10. Mason TG, Lin MY (2005) Phys Rev E71 040801(R). DOI 10.1103/PhysRevE.71.040801
11. Seelenmeyer S, Deike I, Rosenfeldt S, Norhausen Ch, Dingenouts N, Ballauff M, Narayanan T, Lindner P (2001) J Chem Phys 114:10471
12. Arleth L, Xia X, Hjelm RP, Wu J, Hu Z (2005) J Polym Sci B Polym Phys 43:849. DOI 10.1002/polb.20375
13. Guillermo A, Cohen Addad JP, Bazile JP, Duracher D, Elaissari A, Pichot C (2000) J Polym Sci B Polym Phys 38:889. DOI 10.1002/(SICI)1099-0488(20000315)38:6<889::AID-POLB9>3.0.CO;2-L
14. Griffiths PC, Stillbs P, Chowdry BZ, Snowden MJ (1995) Colloid Polym Sci 273:405
15. Woodward NC, Chowdhry BZ, Snowden MJ, Leharne SA, Griffiths PC, Winnington AL (2003) Langmuir 19:3202. DOI 10.1021/la020881i
16. McPhee W, Tam KC, Pelton RH (1993) J Colloid Interface Sci 156:24
17. Crowther HM, Vincent B (1998) Colloid Polym Sci 76:46. DOI 10.1007/s003960050207
18. Senff H, Richtering W (2000) Colloid Polym Sci 278:830. DOI 10.1007/s003960000329
19. Hellweg T, Dewhurst CD, Bruckner E, Kratz K, Eimer W (2000) Colloid Polym Sci 278:972. DOI 10.1007/s003960000350
20. Meyer S, Richtering W (2005) Macromolecules 38:1517. DOI 10.1021ma047776v
21. Berndt I, Pedersen JS, Lindner P, Richtering W (2006) Langmuir 22:459. DOI 10.1021/la052463u
22. Ohta H, Ando I, Fujishige S, Kubota K (1991) J Polym Sci B Polym Phys 29:963
23. Tokuhiro T, Amiya T, Mamada A, Tanaka T (1991) Macromolecules 24:2936
24. Zeng F, Tong Z, Feng H (1997) Polymer 38:5539. DOI 10.1016/S0032-3861(97)00118-3
25. Deshmukh MV, Vaidya AA, Kulkarni MG, Rajamonahan PR, Ganapathy S (2000) Polymer 41:7951. DOI 10.1016/S0032-3861(00)00174-9
26. Durand A, Hourdet D, Lafuma S (2000) J Phys Chem B 104:9371. DOI 10.1021/jp993769a S1089-5647(99)03769-4
27. Spevacek J, Geschke D, Ilavsky M (2001) Polymer 42:463. DOI 10.1016/S0032-3861(00)00357-8
28. Spevacek J, Hanykova L, Ilavsky M (2001) Macromol Chem Phys 202:1122. DOI 10.1002/1521-3935(20010401)202:7<1122::AID-MACP1122>3.0.CO;2-2
29. Hanykova L, Spevacek J, Ilavsky M (2001) Polymer 42:8607. DOI 10.1016/S0032-3861(01)00381-0
30. Starovoytova L, Spevacek J, Hanykova L, Ilavsky M (2004) Polymer 45:5905. DOI 10.1016/j.polymer.2004.06.041
31. Spevacek J, Hanykova L, Starovoytova L (2004) Macromolecules 37:7710. DOI 10.1021/ma0486647 S0024-9297(04)08664-4
32. Starovoytova L, Spevacek J, Ilavsky M (2005) Polymer 46:677. DOI 10.1016/j.polymer.2004.11.089
33. Andersson M, Hietala S, Tenhu H, Maunu SL (2006) Colloid Polym Sci (in press). DOI 10.1007/s00396-006-1470-2

34. Wu X, Pelton RH, Tam KC, Woods DR, Hamielec AE (1993) J Polym Sci A Polym Chem 31:957
35. Pelton RH, Pelton HM, Morphesis A, Rowell RL (1989) Langmuir 5:816
36. Daly E, Saunders BR (2000) Langmuir 16:5546. DOI 10.1021/la991292o S0743-7463(99)01292-5
37. Woodward NC, Chowdhry BZ, Leharne SA, Snowden MJ (2000) Eur Polym J 36:1355. DOI 10.1016/S0014-3057(99)00207-4
38. Ding Y, Ye X, Zhang G (2005) Macromolecules 38:904. DOI 10.1021/ma048460q S0024-9297(04)08460-8
39. Grinberg NV, Dubovik AS, Grinberg VY, Kuznetsov DV, Makhaeva EE, Grosberg AY, Tanaka T (1999) Macromolecules 32:1471. DOI 10.1021/ma9810924 S0024-9297(98)01092-4
40. Zhu PW, Napper DH (1996) Colloids Surf A 113:145